
Remote Sensing Letters

ISSN: 2150-704X (Print) 2150-7058 (Online) Journal homepage: www.tandfonline.com/journals/trsl20

# Surface area to volume scaling of alpha shapes and convex hulls fit to lidar derived mangrove island point clouds

Charles A. Price, Monica Papeş, Ioannis Sgouralis & Todd A. Schroeder

REMOTE SENSING LETTERS
2024, VOL. 15, NO. 12, 1259–1269
https://doi.org/10.1080/2150704X.2024.2414434

Taylor & Francis
Taylor & Francis Group

Check for updates

# Surface area to volume scaling of alpha shapes and convex hulls fit to lidar derived mangrove island point clouds

Charles A. Price[a,b], Monica Papeş[a,b], Ioannis Sgouralis[c] and Todd A. Schroeder[d]

[a]Ecology and Evolutionary Biology, University of Tennessee, Knoxville, TN, USA; [b]National Institute for Modelling Biological Systems, University of Tennessee, Knoxville, TN, USA; [c]Department of Mathematics, University of Tennessee, Knoxville, TN, USA; [d]USDA Forest Service, Southern Research Station, Forest Inventory and Analysis, Knoxville, TN, USA

**ABSTRACT**
The importance of mangroves in marine community stability has become increasingly clear. Understanding the factors structuring mangrove communities, how they respond to disturbance, and how much biomass they contain has become a research priority. The study of mangroves using approaches adapted from terrestrial systems is common yet challenging, highlighting the need for novel approaches. In recent years, remote sensing techniques (lidar and photogrammetry) have provided insight into mangrove composition, extent, and size variability. Here, we build upon this previous work by examining the structure of mangrove islands using convex hulls and alpha shapes fit to airborne lidar data obtained from the United States Geological Survey (USGS). We find that across 527 different islands occurring in eight locations around coastal Florida, the scaling properties of these shapes are tightly constrained. Of particular interest is the scaling of surface area to volume, which differs from null models, and is close to the 3/4 scaling predicted by prominent theoretical models. Our results suggest that convex hulls and alpha shapes may be useful models to capture aspects of mangrove island vegetation structure and indicate the need to better understand how plant abundance, size, and biomass contribute to the structure and variability of lidar data.

**ARTICLE HISTORY**
Received 27 April 2024
Accepted 5 October 2024

**KEYWORDS**
Alpha shape; convex hull; mangrove; allometry

## 1. Introduction

In the intertidal zone where the ebb and flow of seawater leaves soils highly saline, few terrestrial plant species can survive. However, a relatively small number of shrub and tree species have adaptations that enable them to tolerate high salt levels (Lugo and Snedaker 1974). This group of species, known as mangroves, includes around 80 species globally (Duke, Ball, and Ellison 1998). Mangrove forests are recognized as critically important habitats for several reasons (Alongi 2002; Friess et al. 2019). First, mangroves serve as nurseries for a plethora of marine species due to the complex structure of their root systems which provide shelter during early vulnerable life

**CONTACT** Charles A. Price cprice9@utk.edu Ecology and Evolutionary Biology, Dabney Hall 1416 Circle Dr, Knoxville, TN 37996-3140, USA
Supplemental data for this article can be accessed online at https://doi.org/10.1080/2150704X.2024.2414434

stages (Nagelkerken et al. 2008; Laegdsgaard and Johnson 2001; Mumby et al. 2004). Second, organic decay rates are low in the anoxic soils, allowing mangrove forests to sequester carbon (Alongi 2012; Lee et al. 2014), with soil carbon levels among the highest in the tropics (Alongi 2012; Donato et al. 2011; Komiyama, Ong, and Poungparn 2008). Finally, mangroves provide a buffer against strong waves and storm surges associated with thunderstorms and hurricanes, protecting coastal areas from erosion and damage (Alongi 2008; Vizcaya-Martínez et al. 2022; Zhang et al. 2012).

Mangroves are also difficult to study. Mangroves frequently occur in areas where shallow water makes boat access challenging, and frequently co-occur with dangerous fauna. A number of mangrove species (*Rhizophora spp*.) have dense prop root systems growing in tidal mud flats that make traversing them quite challenging (Flores-de-Santiago and Flores-Verdugo 2024).

In an effort to increase our understanding of the factors that influence the abundance, distribution, and structure of mangrove forests, many scientists and land managers have turned to remote sensing approaches (Heumann 2011; Kuenzer et al. 2011; Wang et al. 2019). Passive (optical) and active (lidar) remote sensing data collected by satellites, planes, and unmanned aerial vehicles (UAVs or drones) have dramatically increased the information available to characterize mangrove size, biomass, vegetation, distribution, and response to disturbance (Fromard, Vega, and Proisy 2004; Guo et al. 2017; Richards and Friess 2016; Simard et al. 2006, 2019). Methodological approaches that reveal recurrent underlying structural patterns within and across mangrove sites and habitats are of particular interest (Rovai et al. 2021).

Two of the most informative variables with respect to the form and function of forest plants are their surface area and volume. The surface area of plants is a proxy for metabolic and resource flux rates as both the leaves and stems are sites of growth metabolic activity (West, Brown, and Enquist 1999). Plant volume is a proxy for plant mass (both living and dead material) and correlates strongly with resource requirements and the amount of standing carbon. Measuring the surface area and volume of plants using traditional approaches is prohibitively time-consuming. Lidar-based approaches offer the promise of estimating surface area and volume rapidly, however there are many issues to consider.

Geometric properties like surface area and volume of plants can be difficult to characterize exclusively from lidar data (point clouds). This can be due to data limitations such as sparse, missing, or noisy recordings, but primarily because point clouds are only discretized versions of their underlying objects; accurate characterization methods start with a reconstruction step. During reconstruction, individual points in a point cloud are connected with nearby points to form meshes, yielding continuous approximations of the underlying physical object of interest. Subsequently, the geometric properties of the objects are obtained by considering the corresponding properties of the reconstructed meshes. As the reliability of the resulting estimates depends critically on the quality of the applied reconstruction, the question of how best to connect nearby points in a point cloud to obtain repeatable, meaningful reconstructions is an area of current interest. For dense point clouds such as those collected with a terrestrial laser scanner, there are methods available to create meshes, surfaces or shapes (e.g., quantitative structural models) that represent the trunk, branches, and leaves of trees (Calders et al. 2015;

Raumonen et al. 2013). However, lidar data collected from planes or drones usually lack sufficient density, particularly below the canopy, for such approaches to work.

Here, we take two complimentary approaches to reconstruct area and volume from airborne lidar data. The first is to fit a convex hull to each island mangrove represented by a point cloud set. The advantage of using convex hulls is that their shape is unambiguous. There is one unique convex hull for a given set of points. A disadvantage of convex hulls is their convexity. In nature, concave surfaces are commonly found, particulary when analyzing vegetation. To capture the concavity in point clouds we utilize a second method, alpha shapes. Alpha shapes connect points with lines within a predetermined radius, enabling the construction of surfaces and volumes created by triangular sets (Edelsbrunner, Kirkpatrick, and Seidel 1983). A disadvantage of geometries derived from alpha shapes is that for a given set of points, hundreds or thousands of different alpha shapes can be created by varying the radius used to construct them, which begs the question: which radius is best? Moreover, alpha shapes may erroneously connect points from different real-world objects (plants) and thus may under or over represent the object geometries. Despite these limitations, the ability of alpha shape to capture concave surfaces make this method useful for characterizing vegetation area and volume of mangrove islands, as we will illustrate further.

Our main objective was to test the hypothesis that forest patch size predicts forest volume and surface area based on theory for the scaling of surface area and volume in individual trees. We investigated the potential of geometric shapes fit to lidar point clouds of vegetation to estimate forest patch size and volume in mangrove forest islands of varying size. In many mangrove habitats (but not all), species occur in small islands containing anywhere from one to hundreds or thousands of individuals (Serrano et al. 2020). An advantage of working with island-level data is that they have discrete boundaries: where the vegetation starts and stops is clear, and thus their overall size and geometric properties are relatively easy to determine. In contrast, determining the dimensions of groups of trees growing within contiguous forests from airborne or spaceborne lidar introduces issues around whether individual trees and shrubs are inside or outside a given region of interest. This can be extremely difficult to assess from remotely sensed data in systems where tree crowns overlap and trunks are obscured.

We take an allometric approach to examine relationships between size of mangrove islands and variability in the geometry of vegetation area and volume. We utilize this approach to investigate four basic questions about mangrove islands:

(1) Are there systematic changes in the surface area and volume of geometric shapes fit to point clouds derived from mangrove islands of increasing size? If so, how systematic and constrained are those changes?
(2) Do the scaling relationships we observe differ from null model expectations?
(3) Are the results we observe robust to perturbations in point cloud density?
(4) Do relationships between island size and shape area and volume, as revealed through allometric regression slopes, indicate an underlying mechanism?

## 2. Materials and methods

A description of the data source (USGS 3D elevation program (3DEP)), site selection methodology, initial point cloud processing, and null model development can be found in the Supplementary Materials.

To fit convex hulls and alpha shapes to the point cloud file of each mangrove island (Figure S3), we wrote code in Matlab that looped through all the island csv files, fit a convex hull and an alpha shape to each point cloud, and then determined the surface area and volume of each convex hull and alpha shape, as well as the number of points. The radius parameter within the Matlab alpha shape algorithm is automatically determined and represents the tightest fitting alpha shape that encloses all points. Visual inspection of the projected area and 3D (i.e., volume) alpha shapes of vegetation for each island using this radius revealed too many holes, so we added 0.5 to each alpha radius for each island. This value was determined by iteratively varying the radius parameter value and visually inspecting the results.

To determine the projected area of each island, we used only $x$ and $y$ coordinate information, then fit an alpha shape to each collection of planar points using the same alpha radius as for the vegetation volume (3D) calculations. The area of this alpha shape was used to represent the projected area of each island (Figure S3B).

Most (if not all) of the mangrove islands we studied are tidally inundated, and the overwhelming majority had no recorded elevation on US topographic maps, thus we utilized the difference between the maximum and minimum $z$-values (following removal of ground points) for each island as a proxy for maximum vegetation height. Mean height was calculated as the mean $z$-value of the above ground lidar returns.

### 2.1. Regression statistics

Bivariate relationships among variables derived from point clouds were estimated using standardized major axis regression (SMA). Regression exponents were estimated using the freeware program SMATR (Falster, Warton, and Wright 2003). All data were log transformed before regression fitting to meet the regression assumption of homogeneity of variance. Regression functions were fit to both intrasite and intersite relationships.

For intersite relationships, we compared fits between analogous variable sets (see Table 1). When two regressions had the same slope, we examined the data for a shift in intercept.

For the down sampled data (see next section), we performed a slope equivalence test in SMATR to determine if all the slopes for a given allometric relationship were statistically identical.

### 2.2. Robustness analysis

To assess whether our results were robust to perturbations, we randomly down sampled all point clouds by a fixed percentage, in steps of 10 from 90% to 10%. We then repeated the interisland regression statistics for the 16 bivariate relationships of interest (Table 1) to determine if slopes fit to down sampled data clouds differed from the full point cloud sets.

## 3. Results

Lidar data processing and segmentation in CloudCompare resulted in 527 island point clouds across 8 sites. The summary statistics of the surface area and volume of alpha shapes and convex hulls are in Table S2. Regression statistics are in Tables 1 and Table S3.

**Table 1.** Standardized major axis regression statistics for the relationships among variables derived from lidar cloud points with convex hull and alpha shape methods. The figure that corresponds to each relationship is given in the column titled Figure. The mean intrasite slope is given in the final column to allow easy comparison with the intersite slopes. The reader identify pairs of relationships that were evaluated for slope equivalence. InterSlope – interspecific slope, LowCI – lower 95% confidence interval, UppCI – upper 95% confidence interval, Interc – intercept, MeanIntraSlope – mean intraspecific slope.

| $Log_{10}$ *Y* variable | $Log_{10}$ *X* variable | Figure | $R^2$ | InterSlope | LowCI | UppCI | Interc | LowCI | UppCI | SameSlope | SameIntercept | MeanIntraSlope |
|---|---|---|---|---|---|---|---|---|---|---|---|---|
| Alpha Area ($m^2$) | Alpha Volume ($m^3$) | 1(a) | 0.963 | 0.800 | 0.787 | 0.813 | 0.768 | 0.720 | 0.815 | Yes | No | 0.816 |
| Hull Area ($m^2$) | Hull Volume ($m^3$) | 1(b) | 0.987 | 0.790 | 0.783 | 0.798 | 0.498 | 0.468 | 0.529 | | | 0.791 |
| Number of Lidar Points | Alpha Area ($m^2$) | 1(c) | 0.940 | 1.152 | 1.128 | 1.177 | −0.013 | −0.101 | 0.074 | Yes | Yes | 1.064 |
| Number of Lidar Points | Hull Area ($m^2$) | 1(d) | 0.921 | 1.131 | 1.104 | 1.159 | 0.056 | −0.043 | 0.155 | | | 1.050 |
| Number of Lidar Points | Alpha Volume ($m^3$) | 1(e) | 0.913 | 0.922 | 0.899 | 0.945 | 0.871 | 0.787 | 0.955 | Yes | No | 0.867 |
| Number of Lidar Points | Hull Volume ($m^3$) | 1(f) | 0.919 | 0.894 | 0.872 | 0.916 | 0.620 | 0.533 | 0.707 | | | 0.829 |
| Alpha Area ($m^2$) | Projected Area ($m^2$) | S4(a) | 0.996 | 0.970 | 0.965 | 0.975 | 0.544 | 0.527 | 0.561 | No | N/A | 0.976 |
| Hull Area ($m^2$) | Projected Area ($m^2$) | S4(b) | 0.984 | 0.988 | 0.978 | 0.999 | 0.493 | 0.459 | 0.527 | | | 0.991 |
| Alpha Volume ($m^3$) | Projected Area ($m^2$) | S4(c) | 0.955 | 1.213 | 1.191 | 1.235 | −0.279 | −0.350 | −0.209 | No | N/A | 1.205 |
| Hull Volume ($m^3$) | Projected Area ($m^2$) | S4(d) | 0.978 | 1.251 | 1.235 | 1.266 | −0.006 | −0.057 | 0.044 | | | 1.255 |
| Alpha Area ($m^2$) | Hull Area ($m^2$) | S5(a) | 0.983 | 0.982 | 0.971 | 0.993 | 0.060 | 0.020 | 0.099 | N/A | N/A | 0.988 |
| Alpha Volume ($m^3$) | Hull Volume ($m^3$) | S5(b) | 0.972 | 0.970 | 0.956 | 0.984 | −0.273 | −0.329 | −0.218 | N/A | N/A | 0.959 |
| Number of Lidar Points | Projected Area ($m^2$) | S5(c) | 0.946 | 1.118 | 1.096 | 1.140 | 0.614 | 0.543 | 0.685 | N/A | N/A | 1.038 |
| Max Vegetation Height (m) | Mean Vegetation Height (m) | S5(d) | 0.802 | 0.960 | 0.924 | 0.998 | 0.404 | 0.385 | 0.423 | N/A | N/A | 1.047 |
| Mean Vegetation Height (m) | Projected Area ($m^2$) | S5(e) | 0.420 | 0.235 | 0.220 | 0.250 | −0.244 | −0.294 | −0.195 | N/A | N/A | 0.240 |
| Max Vegetation Height (m) | Projected Area ($m^2$) | S5(f) | 0.569 | 0.225 | 0.213 | 0.238 | 0.169 | 0.129 | 0.210 | N/A | N/A | 0.239 |

The smallest island had 63 points and projected area of 13.9 $m^2$. The largest island had 1,805,785 points and a projected area of 210,864 $m^2$. The mean number of points per island was 79,504.

Across all islands, the average number of lidar points was 10.6 points/$m^2$, calculated as the ratio of the number of lidar points to the island projected area. At the quality level QL1, lidar data are expected to have a nominal pulse density of > = 8 points/$m^2$ (2024), thus our results are consistent with that expectation.

The relationships between the variables described in Table 1 are all linear, with low variance around the SMA regression lines. The mean coefficient of determination ($R^2$) for all intersite relationships is 0.891, and the mean for all intrasite relationships is 0.885. Excluding relationships involving plant height (max or mean), the mean intersite $R^2$ is 0.958, and the mean intrasite $R^2$ is 0.963.

Figure 1 and S4 contain pairs of relationships for area and volume of mangrove islands, derived from alpha shapes and convex hulls, island projected area (from alpha shapes), and number of lidar points. For example, Panels A and B in Figure 1 represent a pair. Of these pairs of relationships, the three in Figure 1 had slopes that were not statistically different than one another (Table 1). The pairs of relationships in Figure S4 had slopes that were very close to one another but statistically different (Table 1).

As seen in Figure S5 Panels A and B, the scaling of alpha area to hull area and alpha volume to hull volume is close to isometry, but slightly less. In Figure S5, Panel C we see that the number of points increases faster than the island projected area, likely reflecting the increase in canopy layering that comes with an increase in mean and max height as shown in Panels E and F of Figure S5.

Figure S6 contains the distributions of 100 slopes (each panel) for the allometric relationship between the surface area and volume of alpha shapes and convex hulls fit to randomly distributed points (see Methods). Point clouds drawn from uniform distributions are in Panels A and B. Point clouds drawn from random distributions are in Panels C and D. Point clouds drawn from constrain normal distributions are in Panels E and F.

None of the allometric relationships fit to the down sampled point clouds (Table S5) differed from the full point cloud set (Table S4, $p>>0.05$), save a minor difference in the scaling of alpha volume with hull volume ($p = 0.029$).

## 4. Discussion

Our study examined the area and volume of 527 mangrove islands across a latitudinal gradient spanning over 500 km, covering a variety of soil, climatic, and environmental conditions. We found that the relationships between the surface area and volume of geometric shapes derived from lidar point clouds from mangrove islands all fell along fairly constrained functions (Figure 1, Figure S4, Table 1). Moreover, the slope values of lines of best fit for the relationships between surface area and volume (Figure 1(a,b)) were outside the range of slope values derived from null expectations based on three different types of randomly distributed points (Figure S6), and insensitive to subsampling across the entire range we employed (90–10%). This suggests that these scaling relationships are robust and potentially informative of mangrove forest structure.

Our results indicate that, by simply measuring the projected area of an island, one could predict with reasonable accuracy the volume and surface area of convex hulls or

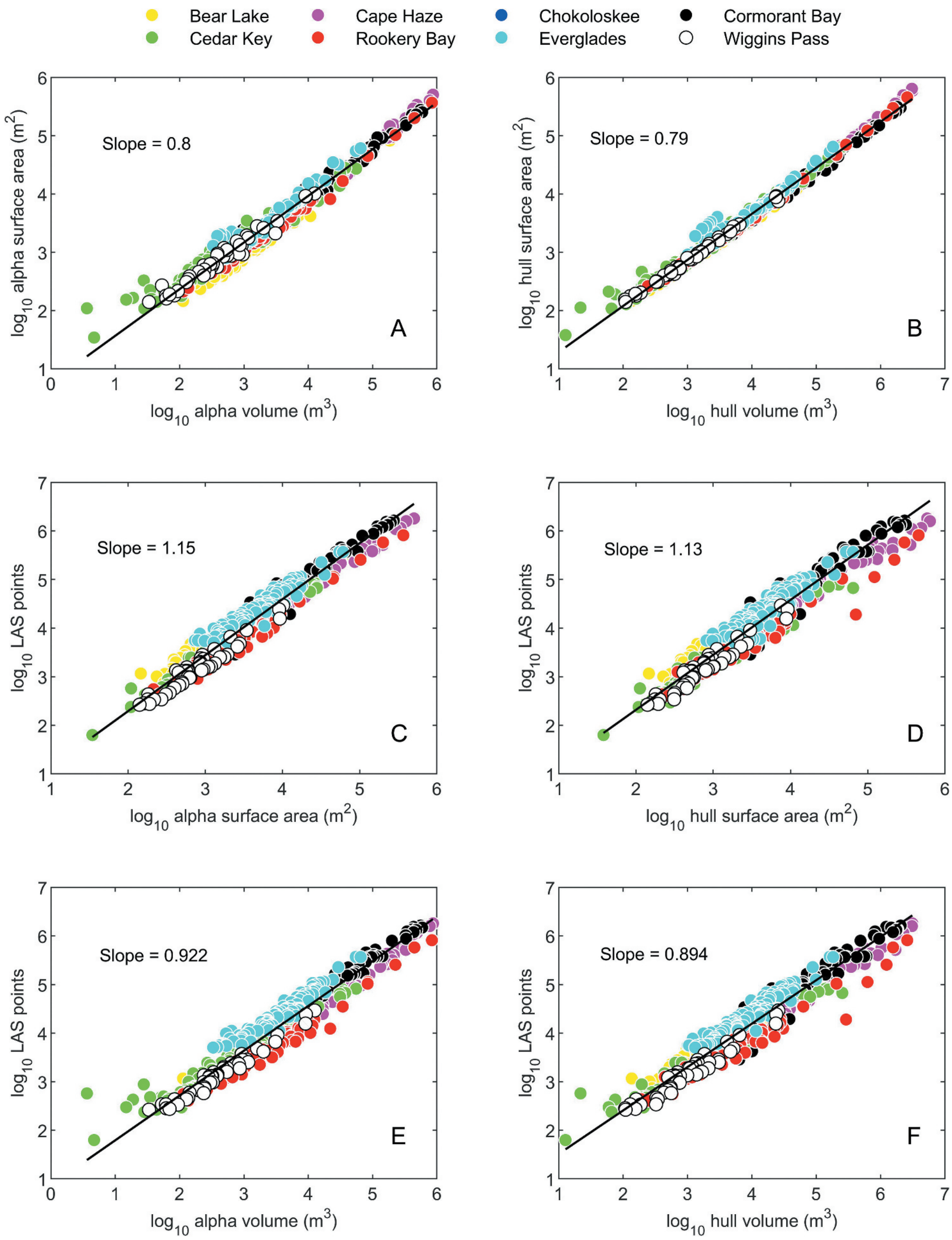


**Figure 1.** Alpha shape, convex hull and point cloud data scaling for mangrove islands in Florida, U.S.A. Scaling relationships between the surface area and volume of alpha shapes (Panel A), the surface area and volume of convex hulls (Panel B), and the number of points with alpha shape and hull area and volume (Panels C-F) for the 527 island point clouds across eight sites. Intersite statistics are given in Table 1 and intrasite statistics in Table S3. Points from each site are colour coded as per the legend.

alpha shapes that enclose their points. What remains to be determined is how well the underlying plant volume and biomass correlate with the convex and concave surfaces we have utilized here (hull and alpha shapes, respectively).

While we derived the alpha shapes and convex hulls from coarse data, numerous published studies utilize the mean height of lidar returns *alone* to estimate biomass in these systems. For example, Simard et al. (2006) and Feliciano et al. (2017) used mean height derived from 30 m and 12 m raster spacings, respectively, to estimate biomass in Everglades National Park. Our approach leverages richer geometric information than these previous studies by examining more of the 3-dimensional canopy structure. To determine the correlation between the geometric shapes and the underlying biomass, one could measure the dimensions of trees (diameter at breast height, tree height), within and across islands, and leverage established allometric relationships (Komiyama, Ong, and Poungparn 2008; Rovai et al. 2021; Smith and Whelan 2006) for the species in these communities to estimate biomass. Combined with area and volume estimates from remotely collected data, one could test the strength of the association between these two approaches.

The slope of the relationship between vegetation area and volume obtained with the two methods, convex hulls and alpha shapes, did not differ from one another, while the intercept was higher for alpha shapes. This is not surprising given that alpha shapes incorporate concavity and thus will typically have a greater surface area. As expected, the vegetation volume of mangrove islands estimated with convex hulls was greater than that estimated with alpha shapes. In fact, as the alpha radius goes to infinity, alpha shapes approach convex hulls. The average vegetation volume estimated with alpha shape was ~43% of the volume estimated with convex hull. Curiously, the average vegetation surface area resulting from alpha shape approach was ~101% of the area from the hull approach (range 13% to 206%, Table S2), so while individual mangrove islands might differ considerably, on average, the two approaches yielded similar surface area estimates.

The slope of the relationship between vegetation volume (alpha or hull) and island projected area was positively allometric (slope >1, Figure S4 C,D). This is likely driven by the fact that larger islands have larger trees (Fig S5 E,F). We are unable to determine the species composition of these islands with lidar data. They all occur in areas dominated by mangroves, and small islands are likely exclusively mangrove species given their tolerance for periodic saltwater inundation. Some of the larger islands may contain larger mangrove individuals in their interior, or even non-mangrove species that attain greater heights. For example, it is common for palm tree species to occur in sandy soils above the water line in habitats that support mangroves in Florida.

It is noteworthy that the slope of the relationship between surface area and volume is close to that predicted by several allometric models for the scaling of plant surface area to volume and different from our null model (Table 1). The well-known fractal model of West, Brown, and Enquist (1999) predicts that the leaf surface area scales with plant volume with an exponent of 3/4 (West, Brown, and Enquist 1999). However, the stem surface area is expected to scale with plant volume with an exponent of 5/8 (=0.625) under their model. In contrast, a more recent theoretical approach, the flow similarity model by Price et al. (2022), predicts that *both* leaf and stem surface area will scale with plant volume with an exponent of 3/4. In our study, we were not able to differentiate between lidar points from leaves versus those from stems. It is likely that both are included in the point clouds we used here, with far more lidar points likely from leaves given the density of plant canopies in mangrove forests. Improvements in approaches that enable separation of leaf and stem surface area within finer scale data, for example from terrestrial lidar scans (compared to airborne lidar), may eventually enable such determination (Hui et al. 2021; Vicari et al. 2019).

We have shown that the geometric properties of convex hulls and alpha shapes fit to remotely sensed lidar data exhibit scaling relationships based on mangrove island size that have low variance and slope values that differ from expectations based on simple null models and are robust to changes in point cloud density. Further, the values of the slopes for surface area to volume relationships are close to those predicted from theoretical models for plant allometric relationships. In addition, point cloud properties such as the number of points and the mean and maximum height of trees vary systematically with island size. Whether these relationships hold with higher resolution data remains an important target for future work that may ultimately reveal the extent to which scaling relationships across plant communities of differing size exhibit regular scaling relationships that emerge from underlying patterns in vegetation structure.

## Disclosure statement

No potential conflict of interest was reported by the author(s).

## Funding

The work was supported by the United States Department of Agriculture, Forest Service [22-CR-11330145-047].

## ORCID

Charles A. Price http://orcid.org/0000-0002-4737-9033

## Data availability statement

Five hundred and twenty-seven individual csv files corresponding to the island point clouds analysed in this paper are freely available in the following Dryad repository:

Price, Charles (Forthcoming 2024). Point cloud coordinates for 527 mangrove islands [Dataset]. Dryad. https://doi.org/10.5061/dryad.vmcvdnd0z

## References

3DEP, USGS. 2024. "Topographic Data Quality Levels (QLs)." https://www.usgs.gov/3d-elevation-program/topographic-data-quality-levels-qls.

Alongi, D. M. 2002. "Present State and Future of the world's Mangrove Forests." *Environmental Conservation* 29 (3): 331–349. https://doi.org/10.1017/s0376892902000231.

Alongi, D. M. 2008. "Mangrove Forests: Resilience, Protection from Tsunamis, and Responses to Global Climate Change." *Estuarine, Coastal and Shelf Science* 76 (1): 1–13. https://doi.org/10.1016/j.ecss.2007.08.024.

Alongi, D. M. 2012. "Carbon Sequestration in Mangrove Forests." *Carbon Management* 3 (3): 313–322. https://doi.org/10.4155/cmt.12.20.

Calders, K., G. Newnham, A. Burt, S. Murphy, P. Raumonen, M. Herold, D. Culvenor, et al. 2015. "Nondestructive Estimates of Above-Ground Biomass Using Terrestrial Laser Scanning." *Methods in Ecology and Evolution* 6 (2): 198–208. https://doi.org/10.1111/2041-210X.12301.

Donato, D. C., J. B. Kauffman, D. Murdiyarso, S. Kurnianto, M. Stidham, and M. Kanninen. 2011. "Mangroves Among the Most Carbon-Rich Forests in the Tropics." *Nature Geoscience* 4 (5): 293–297. https://doi.org/10.1038/ngeo1123.

Duke, N., M. Ball, and J. Ellison. 1998. "Factors Influencing Biodiversity and Distributional Gradients in Mangroves." *Global Ecology and Biogeography Letters* 7 (1): 27–47. https://doi.org/10.1111/j.1466-8238.1998.00269.x.

Edelsbrunner, H., D. Kirkpatrick, and R. Seidel. 1983. "On the Shape of a Set of Points in the Plane." *IEEE Transactions on Information Theory* 29 (4): 551–559. https://doi.org/10.1109/TIT.1983.1056714.

Falster, D. S., D. I. Warton, and I. J. Wright. 2003. "(S)MATR: Standardised Major Axis Tests and Routines." Version 1.0. https://www.bio.mq.edu.au/ecology/SMATR.

Feliciano, E., S. Wdowinski, M. Potts, S.-K. Lee, and L. Fatoyinbo. 2017. "Estimating Mangrove Canopy Height and Above-Ground Biomass in the Everglades National Park with Airborne LiDAR and TanDEM-X Data." *Remote Sensing* 9:702. https://doi.org/10.3390/rs9070702.

Flores-de-Santiago, F., and F. Flores-Verdugo. 2024. "A Comparison of Forest Structural Methods of Semiarid Mangrove Species Using a Field-Based Approach." *Ciencias Marinas* 50. https://doi.org/10.7773/cm.y2024.3432.

Friess, D. A., K. Rogers, C. E. Lovelock, K. W. Krauss, S. E. Hamilton, S. Yip Lee, R. Lucas, J. Primavera, A. Rajkaran, and S. Shi. 2019. "The State of the World's Mangrove Forests: Past, Present, and Future." *Annual Review of Environment and Resources* 44 (1): 89–115. https://doi.org/10.1146/annurev-environ-101718-033302.

Fromard, F., C. Vega, and C. Proisy. 2004. "Half a Century of Dynamic Coastal Change Affecting Mangrove Shorelines of French Guiana. A Case Study Based on Remote Sensing Data Analyses and Field Surveys." *Marine Geology* 208 (2–4): 265–280. https://doi.org/10.1016/j.margeo.2004.04.018.

Guo, M., J. Li, C. L. Sheng, J. W. Xu, and L. Wu. 2017. "A Review of Wetland Remote Sensing." *Sensors* 17 (4). https://doi.org/10.3390/s17040777.

Heumann, B. W. 2011. "Satellite Remote Sensing of Mangrove Forests: Recent Advances and Future Opportunities." *Progress in Physical Geography-Earth and Environment* 35 (1): 87–108. https://doi.org/10.1177/0309133310385371.

Hui, Z., S. Jin, Y. Xia, L. Wang, Y. Yevenyo Ziggah, and P. Cheng. 2021. "Wood and Leaf Separation from Terrestrial LiDAR Point Clouds Based on Mode Points Evolution." *Isprs Journal of Photogrammetry & Remote Sensing* 178:219–239. https://doi.org/10.1016/j.isprsjprs.2021.06.012.

Komiyama, A., J. E. Ong, and S. Poungparn. 2008. "Allometry, Biomass, and Productivity of Mangrove Forests: A Review." *Aquatic Botany* 89 (2): 128–137. https://doi.org/10.1016/j.aquabot.2007.12.006.

Kuenzer, C., A. Bluemel, S. Gebhardt, T. V. Quoc, and S. Dech. 2011. "Remote Sensing of Mangrove Ecosystems: A Review." *Remote Sensing* 3 (5): 878–928. https://doi.org/10.3390/rs3050878.

Laegdsgaard, P., and C. Johnson. 2001. "Why Do Juvenile Fish Utilise Mangrove Habitats?" *Journal of Experimental Marine Biology and Ecology* 257 (2): 229–253. https://doi.org/10.1016/s0022-0981(00)00331-2.

Lee, S. Y., J. H. Primavera, F. Dahdouh-Guebas, K. McKee, J. O. Bosire, S. Cannicci, K. Diele, et al. 2014. "Ecological Role and Services of Tropical Mangrove Ecosystems: A Reassessment." *Global Ecology & Biogeography* 23 (7): 726–743. https://doi.org/10.1111/geb.12155.

Lugo, A. E., and S. C. Snedaker. 1974. "The Ecology of Mangroves." *Annual Review of Ecology and Systematics* 5 (1): 39–64. https://doi.org/10.1146/annurev.es.05.110174.000351.

Mumby, P. J., A. J. Edwards, J. E. Arias-Gonzalez, K. C. Lindeman, P. G. Blackwell, A. Gall, M. I. Gorczynska, et al. 2004. "Mangroves Enhance the Biomass of Coral Reef Fish Communities in the Caribbean." *Nature* 427 (6974): 533–536. https://doi.org/10.1038/nature02286.

Nagelkerken, I., S. J. M. Blaber, S. Bouillon, P. Green, M. Haywood, L. G. Kirton, J. O. Meynecke, et al. 2008. "The Habitat Function of Mangroves for Terrestrial and Marine Fauna: A Review." *Aquatic Botany* 89 (2): 155–185. https://doi.org/10.1016/j.aquabot.2007.12.007.

Price, C. A., P. Drake, E. J. Veneklaas, and M. Renton. 2022. "Flow Similarity, Stochastic Branching, and Quarter Power Scaling in Plants." *Plant Physiology*. https://doi.org/10.1093/plphys/kiac358.

Raumonen, P., M. Kaasalainen, M. Åkerblom, S. Kaasalainen, H. Kaartinen, M. Vastaranta, M. Holopainen, M. Disney, and P. Lewis. 2013. "Fast Automatic Precision Tree Models from Terrestrial Laser Scanner Data." *Remote Sensing* 5 (2): 491–520.

Richards, D. R., and D. A. Friess. 2016. "Rates and Drivers of Mangrove Deforestation in Southeast Asia, 2000-2012." *Proceedings of the National Academy of Sciences of the United States of America* 113 (2): 344–349. https://doi.org/10.1073/pnas.1510272113.

Rovai, A., R. Twilley, E. Castañeda-Moya, S. Midway, D. Friess, C. Trettin, J. Bukoski, et al. 2021. "Macroecological Patterns of Forest Structure and Allometric Scaling in Mangrove Forests." *Global Ecology & Biogeography* 30. https://doi.org/10.1111/geb.13268.

Serrano, D., F. Flores-Verdugo, E. Ramírez-Félix, J. M. Kovacs, and F. Flores-de-Santiago. 2020. "Modeling Tidal Hydrodynamic Changes Induced by the Opening of an Artificial Inlet within a Subtropical Mangrove Dominated Estuary." *Wetlands Ecology and Management* 28 (1): 103–118. https://doi.org/10.1007/s11273-019-09697-w.

Simard, M., L. Fatoyinbo, C. Smetanka, V. H. Rivera-Monroy, E. Castaneda-Moya, N. Thomas, and T. Van der Stocken. 2019. "Mangrove Canopy Height Globally Related to Precipitation, Temperature and Cyclone Frequency." *Nature Geoscience* 12 (1): 40±. https://doi.org/10.1038/s41561-018-0279-1.

Simard, M., K. Q. Zhang, V. H. Rivera-Monroy, M. S. Ross, P. L. Ruiz, E. Castaneda-Moya, R. R. Twilley, and E. Rodriguez. 2006. "Mapping Height and Biomass of Mangrove Forests in Everglades National Park with SRTM Elevation Data." *Photogrammetric Engineering & Remote Sensing* 72 (3): 299–311. https://doi.org/10.14358/pers.72.3.299.

Smith, T. J., and K. R. T. Whelan. 2006. "Development of Allometric Relations for Three Mangrove Species in South Florida for Use in the Greater Everglades Ecosystem Restoration." *Wetlands Ecology and Management* 14 (5): 409–419. https://doi.org/10.1007/s11273-005-6243-z.

Vicari, M. B., M. Disney, P. Wilkes, A. Burt, K. Calders, and W. Woodgate. 2019. "Leaf and Wood Classification Framework for Terrestrial LiDAR Point Clouds." *Methods in Ecology and Evolution* 10 (5): 680–694. https://doi.org/10.1111/2041-210X.13144.

Vizcaya-Martínez, D. A., F. Flores-de-Santiago, L. Valderrama-Landeros, D. Serrano, R. Rodríguez-Sobreyra, L. Felipe Álvarez-Sánchez, and F. Flores-Verdugo. 2022. "Monitoring Detailed Mangrove Hurricane Damage and Early Recovery Using Multisource Remote Sensing Data." *Journal of Environmental Management* 320:115830. https://doi.org/10.1016/j.jenvman.2022.115830.

Wang, L., M. Jia, D. Yin, and J. Tian. 2019. "A Review of Remote Sensing for Mangrove Forests: 1956–2018." *Remote Sensing of Environment* 231:111223. https://doi.org/10.1016/j.rse.2019.111223.

West, G. B., J. H. Brown, and B. J. Enquist. 1999. "A General Model for the Structure and Allometry of Plant Vascular Systems." *Nature* 400 (6745): 664–667.

Zhang, K. Q., H. Q. Liu, Y. P. Li, H. Z. Xu, J. Shen, J. Rhome, and T. J. Smith. 2012. "The Role of Mangroves in Attenuating Storm Surges." *Estuarine, Coastal and Shelf Science* 102:11–23. https://doi.org/10.1016/j.ecss.2012.02.021.